arXiv:cond-mat/9711198v1 [cond-mat.stat-mech] 19 Nov 1997

Monte Carlo study of the magnetic critical properties of the two-dimensional Ising fluid

A.L.Ferreira and W.Korneta*
Departamento de Fisica, Universidade de Aveiro,
3800 Aveiro, Portugal.

A two-dimensional fluid of hard spheres each having a spin ± 1 and interacting via short-range Ising-like interaction is studied near the second order phase transition from the paramagnetic gas to the ferromagnetic gas phase. Monte Carlo simulation technique and the multiple histogram data analysis were used. By measuring the finite-size behaviour of several different thermodynamic quantities, we were able to locate the transition and estimate values of various static critical exponents. The values of exponents β/ν and γ/ν are close to the ones for the two-dimensional lattice Ising model. However, our result for the exponent $\nu = 1.35$ is very different from the one for the Ising universality class.

I. INTRODUCTION

Models with coupled translational and spin degrees of freedom attracted recently considerable attention because they can describe several phenomena in amorphous ferromagnets [1], dilute magnetic alloys and dipolar liquids [2,3]. Spins in such systems are not localized on lattice sites but are able to move. The systems with coupled spin and translational degrees of freedom exhibit a rich variety of phase transitions. Their phase diagrams were determined using the mean spherical approximation, the mean-field theory, density functional methods and Monte Carlo (MC) simulation techniques [1–4]. However the critical behaviour and universality near phase transitions in these systems attracted only little attention. In ref. [5] the critical properties of the Heisenberg fluid near magnetic order-disorder transition were studied by MC simulations. The obtained critical exponents differ by a small but significant amount from the ones for the lattice Heisenberg model. The spin fluid systems resemble lattice-based spin models with annealed site dilution. The Blume-Capel model is an example of the lattice-based Ising model with an annealed site dilution [6]. The density of annealed sites in this model is, however, not fixed but can fluctuate around an average.

The phase diagram of the 2d Ising fluid studied in this paper obtained within the mean-field approximation described in the ref. [4] is shown in figure 1. For high temperatures and low densities there exists critical line separating a paramagnetic gas phase from a ferromagnetic gas phase. The critical line finishes at lower temperatures at the tricritical point. The similar phase diagram was obtained in the 2d Blume-Capel model. Recently MC simulations were used to investigate the tricritical point properties of a 2d Ising fluid and 2d Blume-Capel model [7]. It was shown that both models belong to the same tricritical universality class.

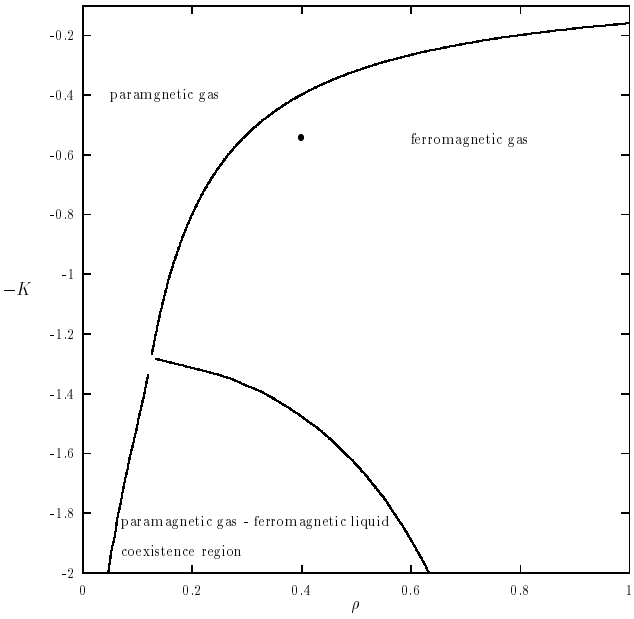


FIG. 1. Mean-field phase diagram for the Ising fluid with the coupling constant K and the density ρ. The line separating the paramagnetic and ferromagnetic gas phases is given by $K = 1/(2\pi\rho)$. The point indicates the location of the phase transition for $\rho = 0.4$ obtained in this paper from MC simulations.

*permanent address : Faculty of Physics, Technical University, Malczewskiego 29, 26-600 Radom, Poland

The aim of this paper is to present the results obtained from MC simulations of the 2d spin fluid with short-range Ising-like interactions near the second-order phase transition from the paramagnetic gas to the ferromagnetic gas phase far from the tricritical point. We performed simulations in systems of different sizes at a constant particle density and for four different temperatures. We analyzed our data combining the multiple histogram technique [8] with finite-size scaling (FSS) [9,10] to obtain estimates for the critical temperature and exponents. In the Sec. II we describe the Ising fluid model and technical aspects of the simulations. Determination of critical exponents and the location of phase transition are given in Secs. III and IV, while Sec.V summarizes our results.

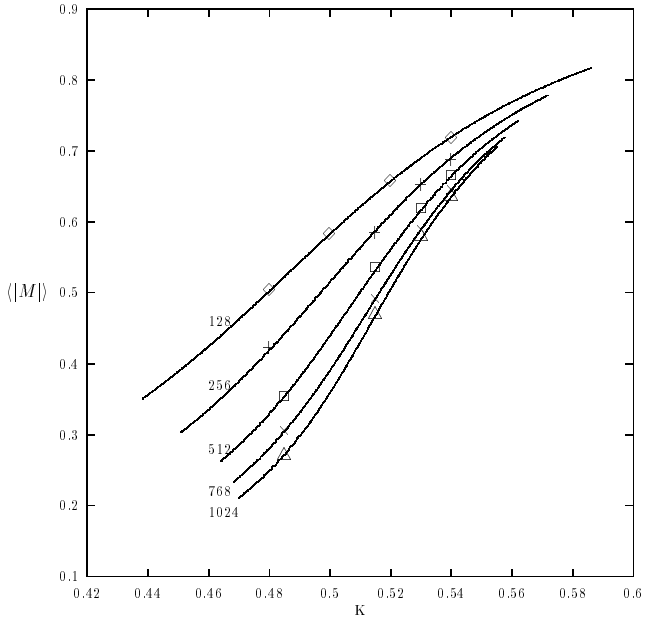


FIG. 2. The magnetization versus the coupling constant K for the five system sizes. The number of particles in the system is indicated. The points are averages over individual simulations. The curves results from the multiple histogram technique. Error bars are smaller than the symbol size.

II. THE MODEL AND SIMULATION DETAILS

We consider a system which consists of particles of diameter σ in two-dimensional space. The internal degrees of freedom of each particle are described by an Ising spin and there is an exchange coupling between spins given by the Yukawa interaction. The system Hamiltonian is:

$$H = \sum_{i,j} \phi(r_{ij}) S_i \cdot S_j \qquad (1)$$

where the interaction potential has the following form,

$$\phi(r) = \begin{cases} \infty & \text{if } r < \sigma \\ -K \ \frac{\sigma}{r} \ \exp(-(r-\sigma)/\sigma) & \text{if } r \geq \sigma \end{cases} \qquad (2)$$

The parameter K is the ratio of the coupling energy to the thermal energy. In this paper we consider the ferromagnetic case ($K > 0$).

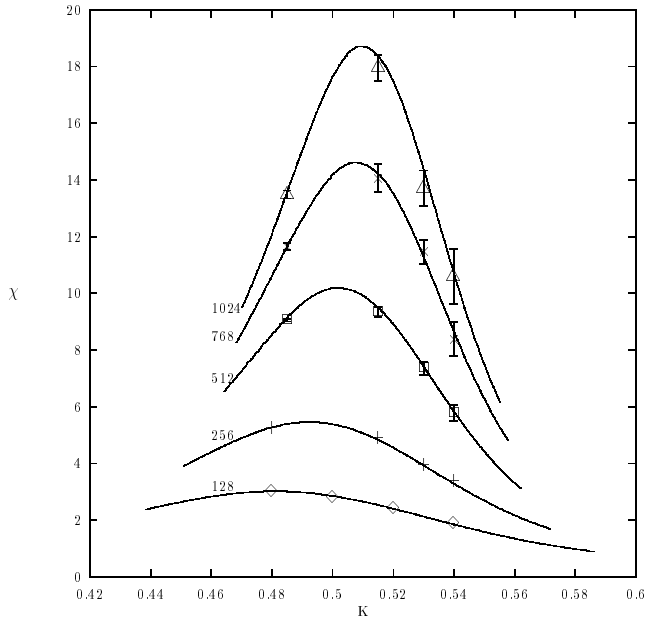


FIG. 3. The magnetic susceptibility versus the coupling constant K for the five system sizes. The number of particles in the system is indicated. The points are averages over individual simulations. The curves results from the multiple histogram technique. Error bars are omitted when smaller than the symbol size.

The MC simulations were performed at a constant particle density $\rho = 0.4$. We studied five systems with the number of particles N equal to 128, 256, 512, 768 and 1024. The periodic boundary conditions and the minimum image convention were applied during simulations [11]. The interaction potential $\phi(r)$ was cut at a distance 6.3246σ. This value was chosen in order to divide the simulation cell into 16 sub-cells for the system with 256 particles. In order to speed up simulations we used the method of linked lists of neighbours [11]. We applied the same simulation algorithm as it is described in ref. [3]. In the present work we have not included any long–range correction to the cuttof procedure as it was done in [3]. The maximum position displacement of particles was chosen in such a way, that the acceptance ratio of the trial moves was around 0.5. The number of MCS/N (Monte Carlo steps per particle) discarded at the beginning of the simulation was larger than 10^4. For each system size the simulations were performed for four values of the parameter K. These values were the following: $K = 0.48, 0.5, 0.52$ and 0.54 for a system with 128 particles, $K = 0.48, 0.515, 0.53$ and 0.54 for a system with 256 particles and $K = 0.485, 0.515, 0.53$ and 0.54 for systems with 512,768 and 1024 particles. These values of K were chosen, because the range of temperatures

where reliable extrapolation of the behaviour of physical quantities could be performed included positions of the maxima of specific heat and magnetic susceptibility and the position of the phase transition in the bulk system. The data were stored at intervals of 10 MCS/N and the total number of updates was $2 \cdot 10^6$ MCS/N for every K value.

Let's denote by M the magnetization per particle of the system defined as $M = (\sum_i Si)/N$. We study critical behaviour of the following quantities [12,13]: the mean absolute value of the magnetization $< |M| >$, the magnetic susceptibility defined as $\chi = KN(< M^2 > - < |M| >^2)$ the fourth-order magnetization cumulant defined as $U = 1 - < M^4 > /(3 < M^2 >)$, the mean energy of the system $< H >$ and the specific heat $C_V = (< H^2 > - < H >^2)/N$, where $< ... >$ denotes canonical ensemble average. We also consider the quantities like the derivatives $\partial \ln < |M| > /\partial K$ and $\partial \ln < M^2 > /\partial K$. In the Heisenberg fluid [5] and 3d lattice Ising model [13] these derivatives were used to extract the critical exponent ν.

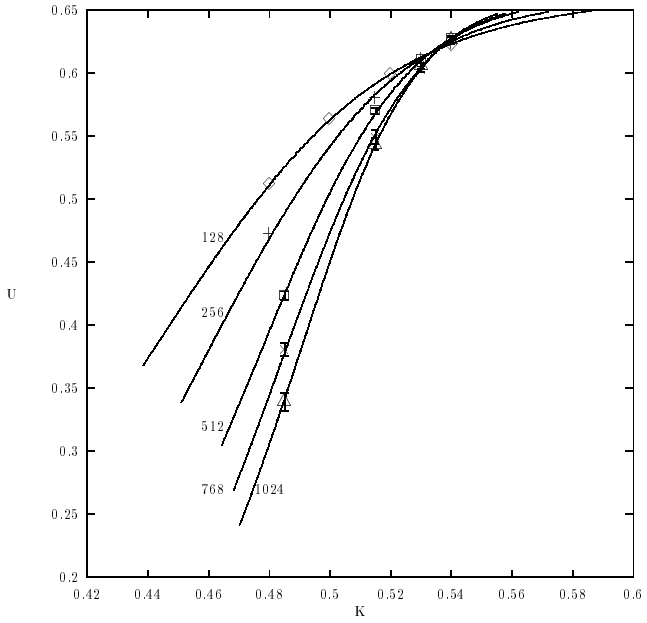


FIG. 4. The fourth-order magnetization cumulant versus the coupling constant K for the five system sizes. The number of particles in the system is indicated. The points are averages over individual simulations. The curves results from the multiple histogram technique. Error bars are omitted when smaller than the symbol size.

The thermodynamic properties of a system, in a wide temperature range, can be obtained by performing several MC simulations at different temperatures and combining them by the application of the multiple histogram technique [8]. This technique allows reliable extrapolation of MC results to the values of K where the interesting positions of the maxima shown by some of the quantities defined above are located. In figures 2, 3 and 4 we show the dependence of quantities $< |M| >$, χ and U on K. The results obtained directly from MC simulations performed at selected K values are also shown in these figures by points. The error bars were obtained by calculating block averages of $10^5 MCS/N$ data points and computing the standard deviation from these block averages. One can notice that the multiple histogram extrapolations are within calculated error bars.

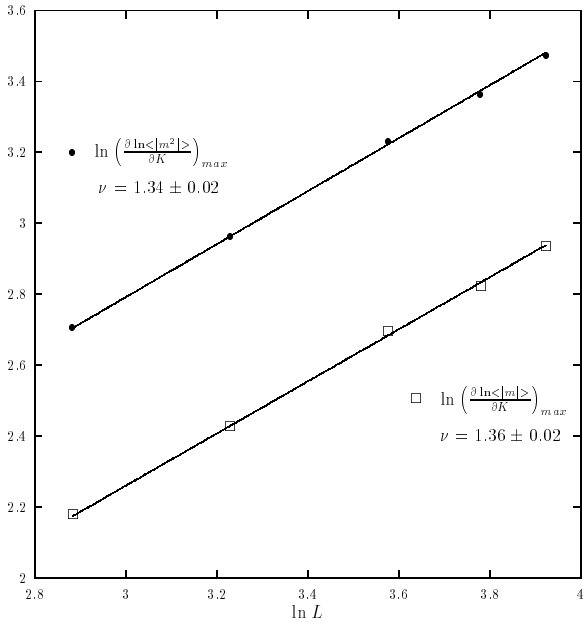


FIG. 5. The plot of the maxima of $\frac{\partial \ln<|M|>}{\partial K}$ and $\frac{\partial \ln<M^2>}{\partial K}$ versus the linear system size L. Error bars are smaller than the symbol size. The straight lines are fits to the data. Their slope is $1/\nu$. The obtained values of the exponent ν are indicated.

III. ESTIMATES OF THE EXPONENT ν AND THE LOCATION OF THE PHASE TRANSITION IN THE BULK SYSTEM

The critical exponent ν characterizing the divergence of the correlation length near the second-order phase transition [10] can be extracted by considering the scaling behaviour of the derivatives $\partial \ln < |M| > /\partial K$ and $\partial \ln < M^2 > /\partial K$ [5,13]. These derivatives can easily be computed using the following identity:

$$\frac{\partial < |M^n| >}{\partial K} = -\frac{1}{K}\left(< |M^n| H > - < |M^n| >< H >\right) \tag{3}$$

Let's denote by L the length of one side of the simulation box. In our case $L = \sqrt{N/\rho}$. The dependence of these derivatives on K has the maximum which should scale with the system size as $L^{1/\nu}$. This method of estimation of the exponent ν is very convenient, because

it can be done without any consideration of the critical coupling K_c in the bulk system. We show in the figure 5 maximum values of $\partial \ln < |M| > /\partial K$ and $\partial \ln < M^2 > /\partial K$ in systems of different sizes together with the fitted straight lines. The goodness of fits Q [14] are $Q = 0.36$ and $Q = 0.32$ for the derivative of $\ln < |M| >$ and $ln < M^2 >$ respectively. The slope of these lines provides estimates for ν, and we obtained $\nu = 1.36 \pm 0.02$ for the maxima of $\partial \ln < |M| > /\partial K$ and $\nu = 1.34 \pm 0.02$ for the maxima of $\partial \ln < M^2 > /\partial K$. These values are higher than the value $\nu = 1$ in the two-dimensional lattice Ising model.

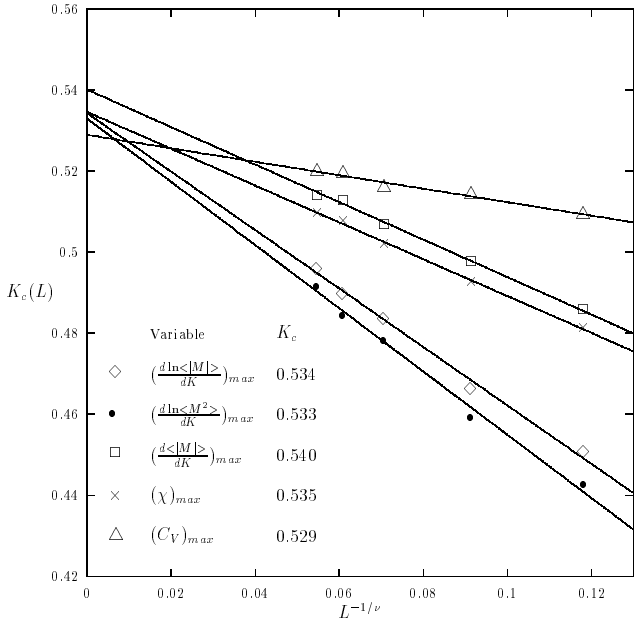


FIG. 6. Size dependence of the location of maxima $K_c(L)$ for several quantities indicated in the figure in finite systems containing 128, 256, 512, 768 and 1024 particles. The straight lines are fits to Eq. 4 with the exponent $\nu = 1.35$. The estimated values of the critical coupling K_c in the bulk system obtained from these fits are shown for each quantity.

The critical coupling K_c in the bulk system is usually determined using the Binder fourth-order magnetization cumulant crossing technique [5,10,13]. Finite size scaling predicts that for sufficiently large systems if we plot U versus K for different choices of L, these curves should have a unique intersection point U^*. The value of K where this occurs is the value of the critical coupling K_c. This value is not biased by any assumptions about critical exponents. For smaller systems there are corrections to FSS and the intersection point between any two curves U vs. K corresponding to systems with side lengths L and L' depends on L and L' [15]. In Table I we give the coordinates of intersection points for different pairs of systems. The values in the table have statistical errors larger than the expected correction terms to FSS. Because of this and a small number of systems studied, we were not able to extract K_c by the extrapolation procedures given in ref. [13].The critical coupling K_c and the intersection value U^* we calculated as the average from the values in the table. We obtained $K_c = 0.535 \pm 0.002$ and $U^* = 0.618 \pm 0.003$. We have excluded from the average the last three rows of the table because for systems with small difference in sizes even a small shift in the cumulant lines can produce a considerable error in the coordinates of intersection points. The estimated common value of the cumulant is only slightly larger than the value $U^* = 0.611 \pm 0.001$ obtained for the two-dimensional lattice Ising model [16].

The value of K_c can also be determined from the size-dependent shifting of the peak of different thermodynamic quantities. In finite systems the quantities like e.g. the specific heat C_V, the magnetic susceptibility χ, $\partial < |M| > /\partial K$, $\partial \ln < |M| > /\partial K$ and $\partial \ln < M^2 > /\partial K$, have maxima as a function of K [9,10,13]. The location of the maximum $K_c(L, A)$ depends both on the system size L and on the quantity A considered. FSS predicts the following dependence of $K_c(L, A)$ on the system size [9,13]:

$$K_c(L, A) = K_c + aL^{-1/\nu} \tag{4}$$

with the omitted corrections to FSS. The constant a depends in magnitude and sign on the particular quantity considered. In order to determine K_c from this equation it is necessary to have both an accurate estimate of the exponent ν and accurate values of $K_c(L, A)$. In figure 6 we plot estimates of $K_c(L, A)$ for different quantities as a function of $L^{-1/\nu}$. The lines in this figure were obtained by the least square fits of the data to Eq. 4 with $\nu = 1.35$, the average of previously determined values. One can notice that values of K_c obtained from the fit agree well with the estimated value $K_c = 0.535$ estimated above from the cumulant intersection points. The value of the exponent ν different than 1.35 will lead, of course, to different estimates of K_c which are inconsistent with the value extracted from cumulant intersection points.

IV. ESTIMATES OF EXPONENT RATIOS β/ν AND γ/ν

The exponent ratio β/ν can be obtained from the finite-size scaling behaviour of $|M|$ either at $K = K_c$ or at the value of K where the derivative $\partial < |M| > /\partial K$ has the maximum. FSS predicts that $|M|$ at these K values should obey the relation $M \sim L^{-\beta/\nu}$. Figure 7 shows the plots corresponding to this relation. The straight lines in this figure were obtained using the least-square fitting routine. The exponent β/ν was determined from the slope of the lines. We obtained: $\beta/\nu = 0.141 \pm 0.005$ ($Q = 0.74$) at K_c and $\beta/\nu = 0.120 \pm 0.006$ ($Q = 0.77$) at the maximum of $\partial < |M| > /\partial K$.

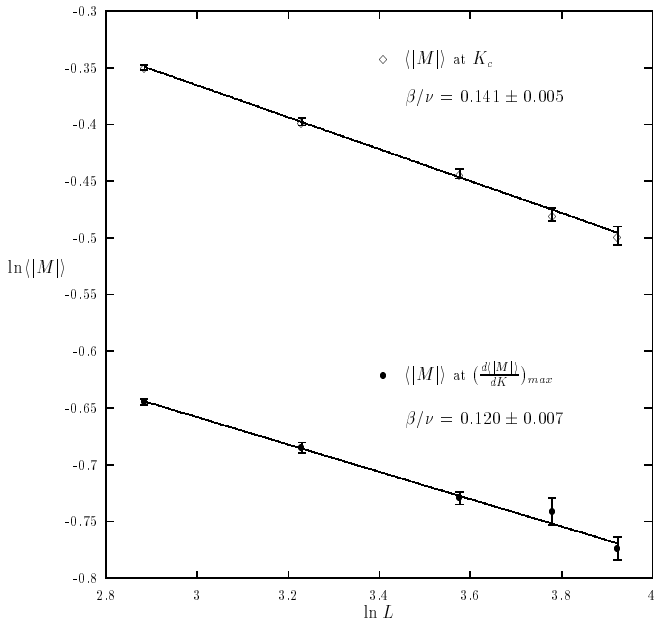


FIG. 7. The plot of the magnetization at the estimated value of the critical coupling in the bulk system $K_c = 0.535$ and at the maximum of $\frac{\partial <|M|>}{\partial K}$, versus the linear system size L. The straight lines are fits to the data. Their slope is $-\beta/\nu$. The obtained values of the ratio of exponents β/ν are indicated.

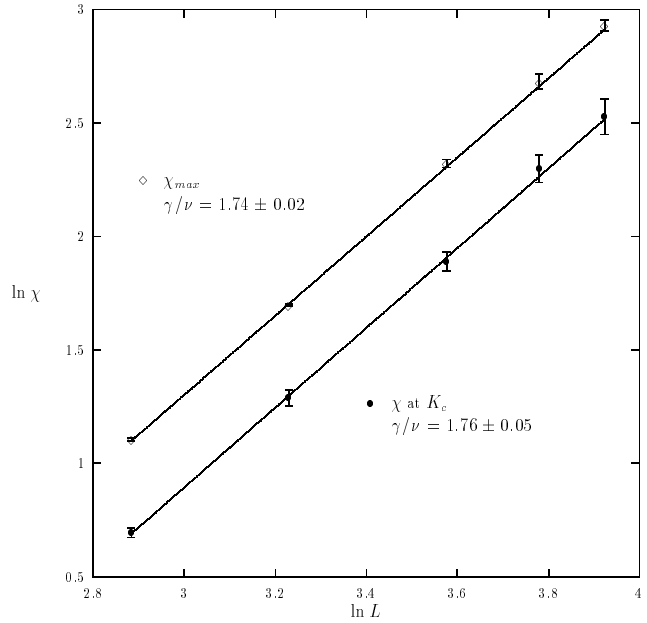


FIG. 8. The plot of the magnetic susceptibility at the estimated value of the critical coupling in the bulk system $K_c = 0.535$ and at the maximum, versus the linear system size L. The straight lines are fits to the data. Their slope is γ/ν. The obtained values of the ratio of exponents γ/ν are indicated.

The exponent ratio γ/ν can be determined from the finite-size scaling behaviour of the maximum of the magnetic susceptibility χ_{max} and of the value $\chi(K_c)$ of the magnetic susceptibility at $K = K_c$. According to FSS these quantities are expected to vary with system size like $L^{\gamma/\nu}$. Figure 8 displays the finite-size scaling behaviour of χ_{max} and $\chi(K_c)$. We estimated the value of the exponent ratio γ/ν from slopes of fitted straight lines. From values χ_{max} we obtained $\gamma/\nu = 1.74 \pm 0.02$ ($Q = 0.31$), whereas from values $\chi(K_c)$ we obtained $\gamma/\nu = 1.76 \pm 0.05$ ($Q = 0.88$).

V. CONCLUSIONS

We have studied the critical behaviour of the two-dimensional Ising fluid at a density $\rho = 0.4$ near the second-order phase transition from the paramagnetic gas to the ferromagnetic gas phase. The multiple histogram technique was applied in order to combine data obtained from four different MC simulations. The largest system we studied consisted of 1024 particles. The critical exponent ν was determined from FSS behaviour of the derivatives $\partial \ln < |M| > /\partial K$ and $\partial \ln < M^2 > /\partial K$. We obtained $\nu \approx 1.35$. This value is much higher than the value $\nu = 1$ obtained for the two-dimensional Ising lattice model. The critical coupling K_c in the bulk system was obtained by considering size-dependent shifting of the maxima of several quantities using the estimated value of the exponent ν. This value was found to be consistent with the location of the fourth-order magnetization cumulant crossing points i.e. with $K_c \approx 0.535$. The estimated common value of the cumulant at $K = K_c$ is $U^* = 0.618$ what is slightly higher than the value $U^* = 0.611$ obtained in the two-dimensional lattice Ising model. All the cumulant intersection values given in table I are above the value 0.611 except the value determined for the pair of systems $[768, 1024]$. As the statistical error increases with the system size and considerable error is expected in the determination of cumulant intersection points for pairs of systems with small difference in sizes we have neglected the last three rows of table I in estimating K_c and U^*. The ratio of critical exponents β/ν and γ/ν we determined from the FSS behaviour of the magnetization and magnetic susceptibility. They are consistent with values obtained in the two-dimensional lattice Ising model. In annealed diluted magnets the exponents are renormalized if the pure specific-heat exponent α is positive and do not change if it is negative [17]. As for the pure lattice Ising model $\alpha = 0$, we expect for the annealed diluted Ising models the pure Ising exponents. Our results disagree with this prediction and suggests a renormalization of exponents which leaves β/ν and γ/ν unchanged and changes ν. We were unable to consider large system sizes with good statistics to determine possible corrections to finite-size scaling. However, the presented self-consistency in the determination of K_c using the estimated exponent ν convinces one that the

obtained values of ν and K_c are correct.

A behaviour similar to ours was reported in studies of the two-dimensional quenched site diluted Ising model [18]. These studies suggest that the ν exponent and the Binder cumulant value, U^* increases with the degree of disorder. These was interpreted as the verification of the weak universality scenario [19] also seen to apply to other models [18]. We plan to study our model with different densities to see if the measured exponents approach the pure Ising values with increasing density.

TABLE I. The values of fourth-order magnetization cumulant $U_{cross}(N_1, N_2)$ and the coupling $K_{cross}(N_1, N_2)$ at the intersection point for different pairs of systems $[N_1, N_2]$ having N_1 and N_2 particles.

$[N_1, N_2]$	$K_{cross}(N_1, N_2)$	$U_{cross}(N_1, N_2)$
[128, 256]	0.5327	0.6153
[128, 512]	0.5331	0.6158
[128, 768]	0.5364	0.6193
[128, 1024]	0.5358	0.6186
[256, 512]	0.5334	0.6164
[256, 768]	0.5380	0.6224
[256, 1024]	0.5368	0.6209
[512, 768]	0.5449	0.6336
[512, 1024]	0.5398	0.6269
[768, 1024]	0.5324	0.6105

ACKNOWLEDGMENTS

W.K. thanks the Junta Nacional de Investigação Científica e Tecnológica in Portugal (JNICT) for the grant under the program PRAXIS XXI, and Professor S.K.Mendiratta for his kind hospitality at the University of Aveiro. A. L Ferreira thanks JNICT for support under PRAXIS2/2.1/FIS/299/94. The references [18] and [19] were pointed out to us by M. A. Santos after the first version of the paper was completed.

[1] N.E.Frankel and C.J.Thompson, J.Phys.C 8 (1975) 3194.

[2] J.M.Tavares, M.M.Telo da Gama, P.I.C.Teixeira, J.J.Wies and M.J.P.Nijmeijer, Phys.Rev.E52 (1995) 1915.

[3] E.Lomba,J.J.Weis, N.G.Almarza, F.Bresme and G.Stell, Phys.Rev.E49 (1994) 5169.

[4] P.C.Hemmer and D.Imbro, Phys.Rev.A16 (1977) 380.

[5] M.J.Nijmeijer and J.J.Weis, Phys.Rev.E53 (1996) 591.

[6] T.W.Burkhardt and H.J.F.Knops, Phys.Rev.B15 (1977) 1602.

[7] N.B.Wilding and P.Nielaba, Phys.Rev.E53 (1996) 926.

[8] R.H.Swendsen, Physica A 194 (1993) 53.

[9] M.N.Barber, in *Phase Transitions and Critical Phenomena*, edited by C.Domb and J.Lebowitz (Academic, New York,1983) vol.8.

[10] K.Binder, in *Finite Size Scaling and Numerical Simulation of Statistical Systems*, edited by V.Privman (World Scientific) 174.

[11] M.P.Allen and D.J.Tildesley, Computer Simulation of Liquids, Oxford University Press 1987.

[12] K.Binder and D.W.Heermann, Monte Carlo Simulations in Statistical Physics, Springer-Verlag 1992.

[13] A.M.Ferrenberg and D.P.Landau, Phys.Rev. B44 (1991) 5081.

[14] W.H.Press, B.P.Flannery, S.A.Teukolsky and W.T.Vetterling, *Numerical Recipes - The Art of Scientific Computing* (Cambridge University Press 1986).

[15] K.Binder, Z.Phys. B43 (1981) 119.

[16] D.W.Heermann and A.Burkitt, Physica A 162 (1990) 210.

[17] R. B. Stinchcombe, in *Phase Transitions and Critical Phenomena*, edited by C.Domb and J.Lebowitz (Academic Press, New York,1983) vol.7.

[18] J. K. Kim and A. Patrascioiu, Phys. Rev. Lett. 72, (1994) 2785 and R. Kuhn, Phys. Rev. Lett. 73, (1994), 2268

[19] M Suzuki, Prog. Theor. Phys. 51, (1974), 1992